

# Cu<sup>2+</sup> Binds to Phosphatidylethanolamine and Increases Oxidation in Lipid Membranes

Matthew F. Poyton,<sup>†</sup> Anne M. Sendecky,<sup>†</sup> Xiao Cong,<sup>§</sup> and Paul S. Cremer<sup>\*,†,‡</sup>

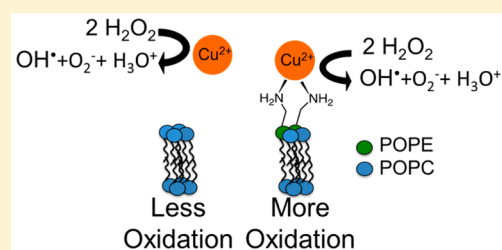
<sup>†</sup>Department of Chemistry, Penn State University, University Park, Pennsylvania 16801, United States

<sup>‡</sup>Department of Biochemistry and Molecular Biology, Penn State University, University Park, Pennsylvania 16801, United States

<sup>§</sup>Department of Chemistry, Texas A&M University, College Station, Texas 77843, United States

**S** Supporting Information

**ABSTRACT:** Herein, we demonstrate that Cu<sup>2+</sup> binds bivalently to phosphatidylethanolamine (PE), the second most abundant lipid in mammalian cells. The apparent equilibrium dissociation constant,  $K_{DApp}$ , for the Cu<sup>2+</sup>–PE complex at physiological pH is approximately 2 μM and is insensitive to the concentration of PE in the membrane. By contrast, at pH 10.0, where PE lipids bear a negative charge,  $K_{DApp}$  decreases with increasing PE content and has a value of 150 nM for bilayers containing 70 mol % PE. The oxidation of double bonds in PE-containing bilayers can be monitored in the presence of Cu<sup>2+</sup>. Strikingly, it was found that the oxidation rate is 8.2 times faster at pH 7.4 for bilayers containing 70 mol % PE than for pure phosphatidylcholine (PC) bilayers upon exposure of both to 70 μM Cu<sup>2+</sup> and 10 mM hydrogen peroxide. The rate of oxidation increases linearly with the PE content in the membrane. These results may help explain the high level of lipid oxidation in PE-containing membranes for neurodegenerative diseases and autism where the Cu<sup>2+</sup> concentration in the body is abnormally high.



## INTRODUCTION

A common hallmark of neurodegenerative diseases and neurological disorders is lipid oxidation.<sup>1</sup> Abnormally high levels of oxidized lipids have been found in the brains of patients with Parkinson's disease, Alzheimer's disease and autism compared with healthy subjects.<sup>1–3</sup> The end products of lipid oxidation, such as malondialdehyde, can react with DNA and are known carcinogens.<sup>4</sup> Determining how lipid oxidation is initiated is vital to our understanding of these diseases. Lipids can be oxidized by reactive oxygen species (ROS) that are produced by a variety of mechanisms, including Fenton-like reactions involving Cu<sup>2+</sup> and hydrogen peroxide.<sup>5</sup> It has been suggested that complexes between lipids and redox-active metal ions might cause increased levels of lipid oxidation.<sup>6–11</sup> Nevertheless, the putative binding sites and their affinities for transition metal ions on cell membranes remain unknown. Exploring this question and elucidating whether membrane-bound transition metal ions can produce ROS and damage the membrane under physiologically relevant conditions are therefore of great importance.

Phosphatidylethanolamine (PE) is the second most abundant lipid in mammalian cells (25% of membrane lipids), and is present at elevated levels in the brain (45% of membrane lipids).<sup>12</sup> It has not historically been considered among the metal-binding lipids, as PE does not bear a negative charge at physiological pH.<sup>13</sup> PE does, however, contain a primary amine that could serve as a ligand for transition metal ions. If these membrane-bound ions could engage in Fenton-like chemistry to produce ROS, then such nascently produced oxidizing agents would be in close proximity to the membrane surface

(Figure 1). ROS, such as hydroxyl radicals, have very short *in vivo* lifetimes.<sup>14</sup> Therefore, it would be much more likely that

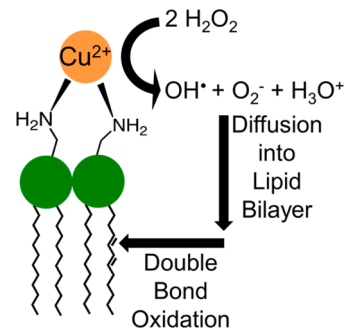


**Figure 1.** Schematic illustration of Cu<sup>2+</sup> binding to the amine moieties on PE head groups. Once bound, Cu<sup>2+</sup> participates in Fenton-like chemistry to produce ROS such as hydroxyl radicals and superoxide, which can oxidize double bonds within the membrane.

such species could damage double bonds on lipid molecules if they are generated directly at the membrane surface, rather than in the bulk solution.

Herein, it is demonstrated that Cu<sup>2+</sup> can bind PE in lipid bilayers and that Cu<sup>2+</sup>–PE complexes can increase the oxidation rate of membrane species in the presence of H<sub>2</sub>O<sub>2</sub>. A reversible fluorescence-quenching assay was employed to

Received: November 4, 2015

Published: January 28, 2016

quantitatively determine the equilibrium dissociation constant for the  $\text{Cu}^{2+}$ –PE complex. It was found that the affinity of  $\text{Cu}^{2+}$  for PE was enhanced as its surface concentration was increased as well as when the bulk pH was increased. Finally, the oxidation of a lipid-bound fluorophore was monitored in small unilamellar vesicles containing different concentrations of PE upon exposure to  $\text{Cu}^{2+}$  and  $\text{H}_2\text{O}_2$ . It was found that the dye was oxidized 8.2 times faster in vesicles containing 70 mol % PE as compared to vesicles made of pure PC lipids. Moreover, the oxidation rate varied linearly with PE concentration.

## RESULTS

**$\text{Cu}^{2+}$  Binds to PE Lipids at Physiological pH and Quenches Fluorophores.** In a first set of experiments,  $\text{Cu}^{2+}$  binding to 1-palmitoyl-2-oleoyl-*sn*-glycero-3-phosphoethanolamine (POPE) was monitored via a fluorescence quenching assay in supported lipid bilayers (SLBs).<sup>15</sup> The lipids in SLBs retain the same fluidity of cellular membranes<sup>16</sup> and the compositions of SLBs can be easily tuned. Such properties make supported bilayers ideal model systems that have been exploited as models of cell membranes to investigate protein and small molecule binding,<sup>17–20</sup> protein aggregation,<sup>21,22</sup> and domain formation.<sup>23</sup> The assays consisted of SLBs coated inside two parallel microfluidic channels (Figure 2A). The

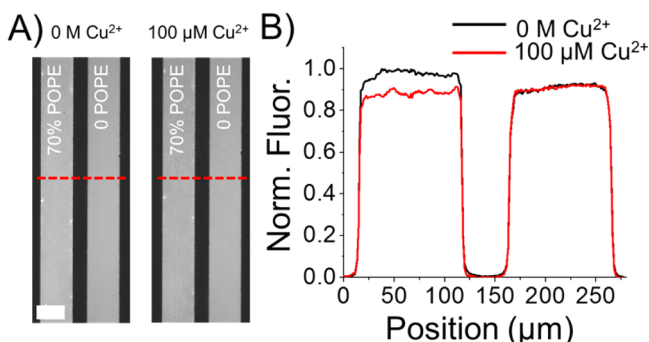


**Figure 2.** (A) Two parallel microfluidic channels containing SLBs with 70 mol % POPE (left channel) and 0 mol % POPE (right channel). The left image in (A) shows a fluorescence micrograph of the bilayers exposed to buffer without  $\text{Cu}^{2+}$ , while the right image shows the same bilayers with  $100 \mu\text{M}$   $\text{Cu}^{2+}$ . (B) Linescans (shown as dashed red lines) across the micrographs in (A). The scale bar at the bottom of the left image is  $100 \mu\text{m}$  in length.

bilayer on the left was made of 70 mol % POPE, 29.5 mol % 1-palmitoyl-2-oleoyl-*sn*-glycero-3-phosphocholine (POPC) and 0.5 mol % Texas Red-DHPE (TR-DHPE), while the one on the right contained 99.5 mol % POPC and 0.5 mol % TR-DHPE. The fluorescence of TR-DHPE was measured in the absence (left image) and presence (right image) of  $100 \mu\text{M}$   $\text{CuCl}_2$  with 10 mM phosphate buffer containing 100 mM NaCl at pH 7.4 and 22 °C. As can be seen, the fluorescence in the SLB containing 70 mol % POPE decreased approximately 10% upon exposure to  $\text{Cu}^{2+}$ , while the fluorescence of the POPC bilayer remained unchanged within experimental error (Figure 2B, linescans of the images from 2A). This quenching phenomenon was not dye specific as  $\text{Cu}^{2+}$  also quenched NBD-PC in membranes containing POPE (Figure S1). Moreover, the lipid tail chemistry was not decisive as it was found that  $\text{Cu}^{2+}$  quenched TR-DHPE in bilayers containing 1,2-dilauroyl-*sn*-glycero-3-phosphoethanolamine (DLPE) (Figure S2). The experiments could also be performed equally well

in buffers other than phosphate (Figure S3). Finally, the bilayers used in these experiments as well as those containing varying concentrations of POPE were two-dimensionally fluid as determined by fluorescence recovery after photobleaching (FRAP)<sup>24,25</sup> (Figure S4) and were shown to be mainly in the liquid crystalline phase by differential scanning calorimetry (DSC) measurements (Figure S5).

The apparent equilibrium dissociation constant ( $K_{\text{DApp}}$ ) of the  $\text{Cu}^{2+}$ –PE complex could be determined by measuring the fluorescence intensity from SLBs as a function of  $\text{Cu}^{2+}$  concentration. Such measurements were made in bilayers with 6 distinct concentrations of POPE ranging from 0 to 70 mol % (Figure 3). As the  $\text{Cu}^{2+}$  concentration in the buffer

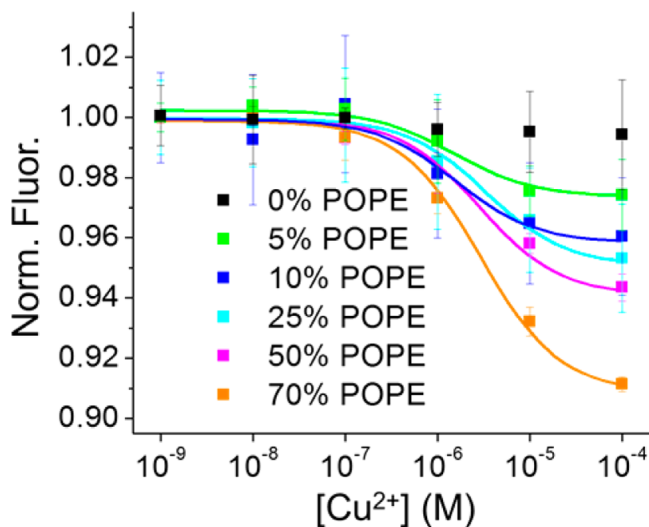


**Figure 3.** Normalized fluorescence intensity (Norm. Fluor.) from SLBs containing 0 to 70 mol % POPE with increasing concentrations of  $\text{Cu}^{2+}$ . The squares are data points and the solid curves represent least-squares fits to Langmuir isotherms. The error bars represent standard deviations from 6 independent measurements.

increased, the fluorescence of the PE-containing bilayers decreased, while the fluorescence from the bilayers that contained no POPE remained nearly constant. The total decrease in fluorescence was largest for SLBs with the highest POPE concentrations. The data for all SLBs were fit to Langmuir isotherms (see SI for fitting procedure) in order to obtain  $K_{\text{DApp}}$  values of the  $\text{Cu}^{2+}$ –PE complex (Table 1). As can be seen, the affinity of  $\text{Cu}^{2+}$  for POPE-containing SLBs was essentially unchanged within error as a function of PE concentration, with an average  $K_{\text{DApp}}$  value of  $2.4 \pm 0.8 \mu\text{M}$  over the entire PE concentration range. While FRAP

**Table 1.**  $K_{\text{DApp}}$  and  $K_{\text{DInt}}$  Values for PE-Containing Bilayers at pH 7.4 and pH 10

mol % PE	$K_{\text{DApp}}$ (M) at pH 7.4	$K_{\text{DApp}}$ (M) at pH 10	$K_{\text{DInt}}$ (M) at pH 10
0	N/A	N/A	N/A
1	N/A	$1.0 \pm 0.4 \times 10^{-5}$	$1.0 \times 10^{-5}$
5	$1.7 \pm 0.5 \times 10^{-6}$	$1.0 \pm 0.4 \times 10^{-6}$	$1.6 \times 10^{-6}$
10	$1.6 \pm 0.9 \times 10^{-6}$	$5.3 \pm 1.0 \times 10^{-7}$	$1.1 \times 10^{-6}$
25	$3.2 \pm 0.5 \times 10^{-6}$	$4.5 \pm 1.0 \times 10^{-7}$	$2.0 \times 10^{-6}$
50	$2.8 \pm 0.7 \times 10^{-6}$	$1.7 \pm 0.2 \times 10^{-7}$	$1.7 \times 10^{-6}$
70	$2.9 \pm 0.5 \times 10^{-6}$	$1.5 \pm 0.2 \times 10^{-7}$	$2.4 \times 10^{-6}$

measurements did show that the bilayers were fluid (Figure S4), DSC measurements suggested that SLBs containing the highest POPE concentration, 70 mol %, had not quite completed the transition into the liquid crystalline phase at 22 °C (Figure S5). As such, the dissociation constant was also measured at 37 °C for SLBs containing 70 mol % POPE, which are completely in the liquid crystalline phase at this temperature (Figure S6). In that case,  $K_{DApp}$  was  $1.5 \pm 0.5 \mu\text{M}$ , which is almost the same within experimental error as the measured  $K_{DApp}$  value at 22 °C. Bilayers containing less POPE had lower gel to liquid crystalline phase transition temperatures and were completely in the liquid crystalline phase at room temperature.<sup>26</sup>

**Dissociation Constant and Quenching Efficiency of  $\text{Cu}^{2+}$ –PE Complexes are pH Dependent.**  $K_{DApp}$  was measured for supported bilayers containing 70 mol % POPE from pH 7.0 to 10.0 (Figure 4A). No apparent binding was noted at pH 7.0 or lower. The data in Figure 4A were fit to Langmuir isotherms to determine  $K_{DApp}$  at each pH and these

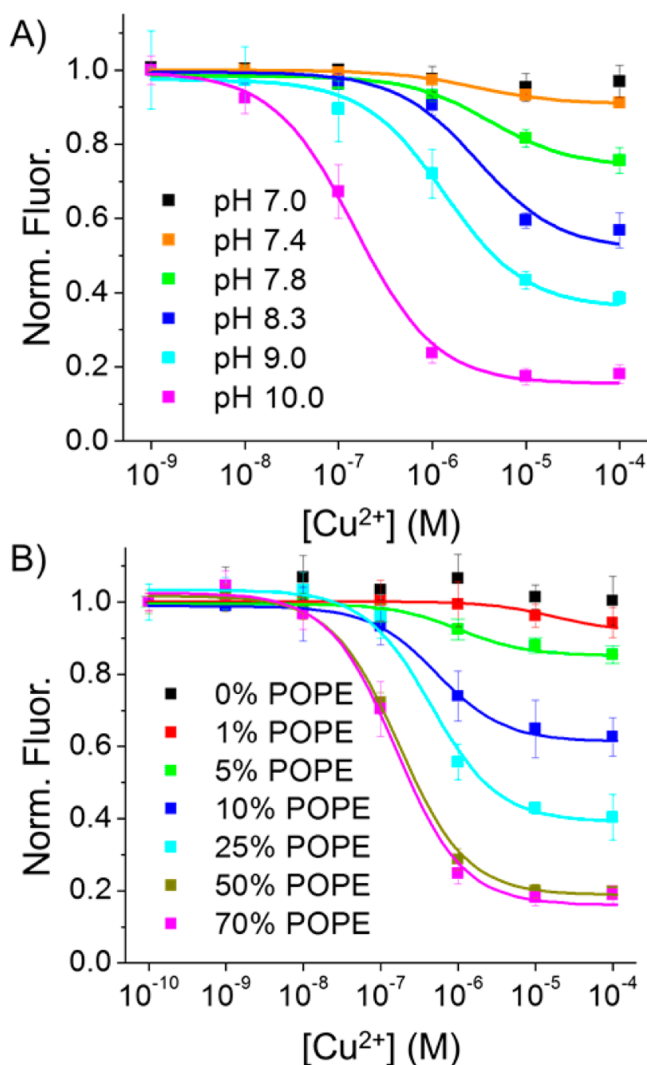


**Figure 4.** (A) Normalized fluorescence intensity from SLBs containing 70 mol % POPE, 29.5 mol % POPC, and 0.5 mol % TR-DHPE from pH 7.0 to 10.0. (B) Normalized fluorescence intensity from SLBs containing 0 to 70 mol % POPE at pH 10.0. The solid lines in each graph represent least-squares fits to a Langmuir isotherm. The error bars represent standard deviations from 6 independent measurements.

values are provided in Table 2. As can be seen, the affinity of  $\text{Cu}^{2+}$  for POPE was pH dependent.  $K_{DApp}$  changed only slightly

**Table 2. Measured  $K_{DApp}$  Values for  $\text{Cu}^{2+}$ –PE in 70 mol % PE Membranes at pH 10.0**

pH	$K_{DApp}$ (M)
7.0	N/A
7.4	$2.9 \pm 0.4 \times 10^{-6}$
7.8	$4.1 \pm 0.9 \times 10^{-6}$
8.3	$3.0 \pm 0.8 \times 10^{-6}$
9.0	$1.3 \pm 0.3 \times 10^{-6}$
10.0	$1.5 \pm 0.2 \times 10^{-7}$

from pH 7.4 to 9.0, falling from 4.1  $\mu\text{M}$  to 1.3  $\mu\text{M}$ ; however, at pH 10.0  $K_{DApp}$  fell more significantly to 150 nM.

The affinity of  $\text{Cu}^{2+}$  for bilayers containing different concentrations of POPE was also measured at pH 10.0 (Figure 4B). As expected, the quenching efficiency increased with increasing POPE content in the bilayers. This occurred because the average distance between a  $\text{Cu}^{2+}$ –PE complex and TR-DHPE decreases as the POPE density increases. More significantly,  $K_{DApp}$  also changed as a function of POPE concentration at this pH, tightening from 10  $\mu\text{M}$  for SLBs containing 1 mol % POPE to 150 nM for SLBs containing 70 mol % POPE (Table 1). This trend is notably different from the behavior at pH 7.4, which showed negligible changes in  $K_{DApp}$  over a wide range of POPE concentrations (Figure 3). This difference arises because PE has an intrinsic  $\text{p}K_a$  of 9.6<sup>27</sup> and bears a net negative charge at pH 10.0. As such, the interfacial charge increases with POPE concentration. This, in turn, leads to an increase in  $\text{Cu}^{2+}$  concentration in the double layer,<sup>28</sup> which causes  $K_{DApp}$  to tighten. By contrast, POPE is mostly protonated at pH 7.4 and therefore zwitterionic near physiological pH. As such, the measured affinity is much less dependent on PE concentration under these conditions.

The effect of surface charge on  $K_{DApp}$  at pH 10.0 can be quantified using Gouy–Chapman theory to model the surface charge corrected affinity ( $K_{DInt}$ ).<sup>13,28,29</sup> In order to properly calculate the surface charge, the stoichiometry of the  $\text{Cu}^{2+}$  complex with POPE must be taken into account. This was measured in 100 nm vesicles containing 70 mol % POPE at pH 10.0 using a method previously employed for  $\text{Cu}^{2+}$ –PS complexes.<sup>15</sup> The results show that most surface bound  $\text{Cu}^{2+}$  ions are bound to two POPE lipids (Figure S7). Next, the surface potential ( $\psi_0$ ) on the membrane was calculated at a concentration of  $\text{Cu}^{2+}$  equal to  $K_{DApp}$ . At this  $\text{Cu}^{2+}$  concentration, half of the POPE lipid binding sites will be occupied and the surface charge will be reduced by half due to the positive charge on the  $\text{Cu}^{2+}$ . This change in surface charge upon  $\text{Cu}^{2+}$  binding was taken into account when calculating  $\psi_0$  (see detailed calculations in the SI and calculated surface potentials in Table S1). The calculated  $\psi_0$  values can then be used to calculate a  $K_{DInt}$  which is independent of surface charge (see detailed calculations in the SI).

The calculated  $K_{DInt}$  values are listed in Table 1. It was found that  $K_{DInt}$  does not change within experimental error for bilayers containing 5 mol % to 70 mol % POPE, averaging  $1.8 \pm 0.5 \mu\text{M}$ . However,  $K_{DInt}$  for membranes containing 1 mol % POPE was almost an order of magnitude weaker. This increased  $K_{DInt}$  value at low POPE concentrations should be the result of predominantly monovalent binding between  $\text{Cu}^{2+}$  and POPE under these conditions. In fact, a similar change in

valency with  $\text{Cu}^{2+}$  has also previously been observed for membranes containing low concentrations of PS lipids.<sup>28</sup> Moreover, it should be noted that the  $K_{\text{DInt}}$  values at pH 10.0 are very similar to the  $K_{\text{DApp}}$  values at pH 7.4. This is consistent with the notion that increased surface charge is predominantly responsible for the apparently tighter binding to POPE lipids that is observed under more basic conditions, rather than a change in the intrinsic affinity of POPE for  $\text{Cu}^{2+}$ .

There was a substantial increase in the depth of quenching at high  $\text{Cu}^{2+}$  concentrations as the pH was raised from 7.4 to 10.0. The fluorescence decreased 82% with 100  $\mu\text{M}$   $\text{CuCl}_2$  at pH 10.0, whereas it only decreased 9% at pH 7.4. Moreover, essentially no quenching was observed at pH 7.0. The change in quenching efficiency should be due to the increase in availability of the  $\text{Cu}^{2+}$ -PE complexes to the TR-DHPE dye as the pH was raised. In fact, fluorescence microscopy shows that 70 mol % POPE bilayers contain microdomains at pH 7.4, while such domains are absent at pH 10.0 (Figure S8). The lateral packing of POPE in vesicles is substantially different from that of POPC, so it is not unexpected that they are segregated from one another in SLBs.<sup>30</sup> The formation of domains at pH 7.4 segregates a substantial portion of the TR-DHPE away from the  $\text{Cu}^{2+}$ -POPE complexes, making the dye unresponsive to them. However, such domains do not form at pH 10.0 as the negatively charged PE lipids repel one another. Finally, the formation of the  $\text{Cu}^{2+}$ -PE complex was found to be completely reversible with changes in pH or upon the addition of EDTA to solution. Cycling the pH between 6.8 and 10.0, for example, resulted in the binding and unbinding of  $\text{Cu}^{2+}$  to the POPE-containing membranes, turning the fluorescence off and on (Figure S9). There was no loss in fluorescence recovery after three cycles of pH changes, demonstrating that the attenuation of fluorescence upon  $\text{Cu}^{2+}$  binding was caused by the metal ion quenching rather than irreversible photo-bleaching.

**Membrane Species are Oxidized More Rapidly in the Presence of  $\text{Cu}^{2+}$ -PE Complexes.** To determine the effect of  $\text{Cu}^{2+}$ -PE complexes on the oxidation rate of membrane-associated species, we monitored the oxidation of a fluorescent probe, C11-BODIPY, in lipid membranes exposed to  $\text{Cu}^{2+}$  and  $\text{H}_2\text{O}_2$ .  $\text{Cu}^{2+}$  can decompose  $\text{H}_2\text{O}_2$  via Fenton-like chemistry to produce hydroxyl radical and superoxide.<sup>31,32</sup> C11-BODIPY is known to be unreactive toward superoxide, but is readily oxidized by hydroxyl radical.<sup>33</sup> The emission wavelength of C11-BODIPY blueshifts from 591 to 520 nm upon oxidation.<sup>34</sup> The fluorescence can be monitored at 591 nm as a function of time in order to measure the rate of dye oxidation.<sup>33,35</sup> These measurements were made at room temperature (22 °C) with 100 nm diameter unilamellar lipid vesicles rather than SLBs, as the dye can occasionally partition out of the lipid membrane. In fact, flowing solution through bilayer-coated microfluidic devices in a heterogeneous assay slowly caused the dye to leach out of the bilayer. Making these measurements in bulk solution avoided this complication.

Figure 5 shows fluorescence emission spectra of phospholipid vesicles containing (A) 0 mol % and (B) 70 mol % POPE (black spectra). These vesicles also contained 0.5 mol % C11-BODIPY and the balance in each case was POPC. The total concentration of lipids for each was 100  $\mu\text{M}$ . Both vesicle samples were exposed to 70  $\mu\text{M}$   $\text{Cu}^{2+}$  and 10 mM  $\text{H}_2\text{O}_2$  in 10 mM Tris and 100 mM NaCl at pH 7.4. After 15 min, the fluorescence peaks decreased in each case (red spectra). This drop, however, was far greater in the presence of POPE. While

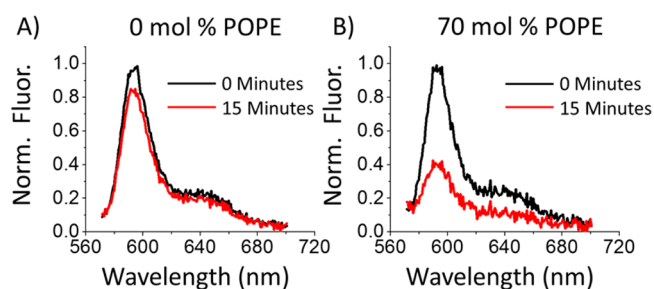


**Figure 5.** Fluorescence emission spectra of C11-BODIPY in lipid vesicle solutions composed of (A) 99.5 mol % POPC and 0.5 mol % C11-BODIPY and (B) 70 mol % POPE, 29.5 mol % POPC, and 0.5 mol % C11-BODIPY. The black lines represent fluorescence spectra taken immediately after the addition of  $\text{H}_2\text{O}_2$  and  $\text{Cu}^{2+}$ , while the red lines are from fluorescence spectra after 15 min have elapsed.

the total amount of copper in each solution was the same,  $\text{Cu}^{2+}$  will be bound to the surface of the vesicles containing 70 mol % POPE. This increased surface concentration of  $\text{Cu}^{2+}$ , in turn, caused a markedly increased oxidation rate.

As can be seen in the spectra above, there are two peaks from C-11 BODIPY corresponding to a Franck-Condon progression.<sup>36</sup> The first one is centered at 594 nm, while the second weaker and broader peak is centered near 620 nm. The attenuation of these peaks, which is similar, can be used to follow the oxidation rate of the dye as a function of time. To do this, we used the normalized area under the 594 nm peak (Normalized  $A_{594}$ ), as its signal-to-noise ratio was superior. The data are plotted over time for vesicles containing various combinations of POPE,  $\text{Cu}^{2+}$ , and  $\text{H}_2\text{O}_2$  (Figure 6). The

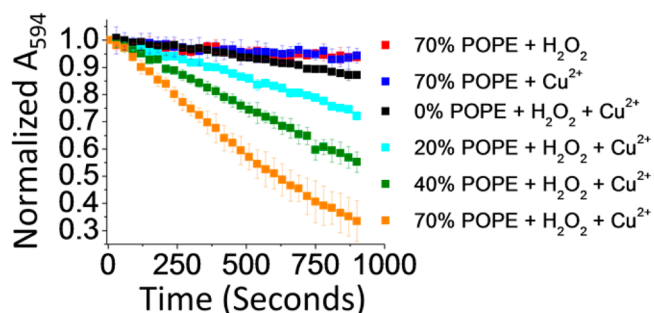


**Figure 6.** Change in the area of the 594 nm peak (Normalized  $A_{594}$ ) as a function of time for the conditions provided in the key. The  $\text{Cu}^{2+}$  and  $\text{H}_2\text{O}_2$  concentrations were 70  $\mu\text{M}$  and 10 mM, respectively, when these species were present.

fluorescence response from vesicles containing 70 mol % POPE decreased 6% over 15 min when exposed to either 10 mM  $\text{H}_2\text{O}_2$  (red squares) or 70  $\mu\text{M}$   $\text{Cu}^{2+}$  (blue squares), individually; however, the fluorescence response fell by 67% when both were present together (orange squares). Moreover, the rate of C11-BODIPY oxidation was dependent on the concentration of POPE in the vesicle. The fluorescence decreased 13% for vesicles containing no PE, and fell to 28% and 55% for vesicles containing 20 mol % and 40 mol % POPE, respectively.

In order to quantitatively determine the rate of oxidation, we assumed that the reaction proceeded via pseudo-first order kinetics. This approximation can be invoked because the concentration of  $\text{H}_2\text{O}_2$  (10 mM) is significantly higher than the 500 nM concentration of C11-BODIPY in bulk solution. Plotting the natural log of the normalized absorption at 594 nm

over time yielded a near-linear trend (Figure S10), which is expected for a pseudo-first order reaction. The apparent rate constant was 8.2 times greater for vesicles containing 70 mol % POPE compared to vesicles containing no PE. A plot of the pseudo first order rate constants is linear against the POPE concentration in the membrane (Figure S11). It should be noted that 10 mM  $\text{H}_2\text{O}_2$  is at least 2 orders of magnitude greater than the  $\text{H}_2\text{O}_2$  concentration under physiological conditions.<sup>37</sup> This high concentration was employed in order to obtain kinetic information under a variety of different conditions on a 15 min time scale, where the fluorimeter was quite stable. Control experiments were also performed with 100  $\mu\text{M}$   $\text{H}_2\text{O}_2$  and 70  $\mu\text{M}$   $\text{Cu}^{2+}$  over 24 h (Figure S12). In this case, the fluorimeter could not be kept running continuously. As expected, however, C11-BODIPY was still oxidized significantly faster in vesicles containing 70 mol % POPE than for vesicles containing 0 mol % POPE and the overall oxidation rate for each case was about 2 orders of magnitude slower than in the presence of 10 mM  $\text{H}_2\text{O}_2$ , which is expected for pseudo-first order kinetics. Oxidation of C11-BODIPY was also measured at 12 and 37 °C for vesicles containing 0 mol % and 70 mol % POPE and 0.5 mol % C11-BODIPY. At these temperatures, the vesicles containing 70 mol % POPE were in the gel and liquid crystalline phases, respectively, while the vesicles containing 0 mol % POPE were in the liquid crystalline phase at both temperatures. While the overall reaction rate was found to be temperature dependent, C11-BODIPY was oxidized 6.7 times faster in vesicles containing 70 mol % POPE than in those without POPE at 37 °C. At 12 °C the difference was a factor of 10 (Figure S13). As such, the specific phase of the bilayer had little if any effect on the rate enhancement of oxidation when POPE was added.

## DISCUSSION

**Physiological Consequences of Oxidation.** The results in Figures 5 and 6 demonstrate that the  $\text{Cu}^{2+}$ -catalyzed decomposition of hydrogen peroxide oxidizes C11-BODIPY faster in vesicles that contain POPE than in those without this lipid. C11-BODIPY has been found to be somewhat more susceptible to oxidation than double bonds on lipid tails.<sup>38</sup> Therefore, the rate of C11-BODIPY oxidation has often been interpreted as a measure of the hydroxyl radical concentration near the membrane surface rather than the absolute expected oxidation rate for particular double bonds on specific lipids of interest.<sup>38</sup> The concentration of  $\text{Cu}^{2+}$  at the membrane surface increases, of course, for vesicles containing POPE because of interfacial binding. Larger rates of C11-BODIPY oxidation demonstrate that this increased local  $\text{Cu}^{2+}$  concentration leads to an increased concentration of ROS at the surface of the vesicle. Such results suggest that  $\text{Cu}^{2+}$  bound to cell membranes could lead to an increase in the concentration of hydroxyl radical near the membrane surface under physiologically relevant conditions, and potentially induce lipid oxidation (Figure 1).

The membranes of neuronal cells can be composed of up to 45% PE lipids.<sup>12</sup> Most PE lipids, however, are on the cytoplasmic leaflet of nonapoptotic cells.<sup>34</sup> The concentration of free  $\text{Cu}^{2+}$  inside of cells is extremely low, perhaps even less than one ion per cell.<sup>35</sup> Therefore, the existence of  $\text{Cu}^{2+}$ -PE lipid complexes in nonapoptotic cells is not likely. Nevertheless, when nerve cells undergo apoptosis, PE flips to the outer leaflet where it is exposed to higher concentrations of labile  $\text{Cu}^{2+}$  in the extracellular environment.<sup>36,37</sup> Therefore,  $\text{Cu}^{2+}$  could bind

to PE in the outer leaflet of apoptotic nerve cells and induce oxidation. Moreover, for individuals with autism or Wilson's disease, the available concentration of  $\text{Cu}^{2+}$  in the body should be higher than in other individuals,<sup>3,8</sup> and the binding of  $\text{Cu}^{2+}$  to PE lipids and subsequent membrane oxidation becomes a greater concern.

While the 8.2 times enhancement of the oxidation rate between vesicles containing 0 mol % POPE and 70 mol % POPE shown in Figure 6 is quite significant, it is possible that the rate enhancement in biological cell membranes may be even greater. Indeed, hydroxyl radicals have a very short *in vivo* lifetime and only diffuse a few molecular lengths before reacting.<sup>39</sup> The lifetime of hydroxyl radicals in the current experiments will be longer than in cells as the model systems contain only a single potential antioxidant, Tris, at low concentration.<sup>40</sup> As a result, oxidation can originate from  $\text{Cu}^{2+}$  ions in the bulk solution in the present experiments, but will be more restricted to surface bound  $\text{Cu}^{2+}$  as the concentration of antioxidants in the bulk is increased. It should also be noted that the enhanced oxidation of lipid membranes in the model systems described above is somewhat analogous to what occurs when redox active metal ions are bound to other biomolecules such as DNA<sup>41-43</sup> or proteins.<sup>44-47</sup> In those cases too, one observes enhanced oxidation. In fact, the oxidation sites on DNA and proteins have been found to be close to the metal ion binding sites.<sup>42,45</sup> For  $\text{Cu}^{2+}$ -PE complexes, this may help explain the increased levels of lipid oxidation found in neurodegenerative diseases, neurodevelopmental disorders, autism, and other copper ion-related diseases.

**Comparison between Phosphatidylethanolamine and Phosphatidylserine Binding to  $\text{Cu}^{2+}$ .** The results described above demonstrate that  $\text{Cu}^{2+}$  can bind to POPE lipids with  $\mu\text{M}$  affinity under physiologically relevant conditions. This is distinct from  $\text{Ca}^{2+}$  and  $\text{Mg}^{2+}$ , which have almost no affinity for PE<sup>13,48</sup> and only bind to the negatively charged moieties on the phosphatidylserine (PS) headgroup.<sup>49,50</sup> The interaction between  $\text{Cu}^{2+}$  and PE is more similar to the binding of  $\text{Cu}^{2+}$  to PS lipids, which also forms a 2 lipid to 1 metal ion complex (Figure 7). Although both lipids contain an amine moiety, the

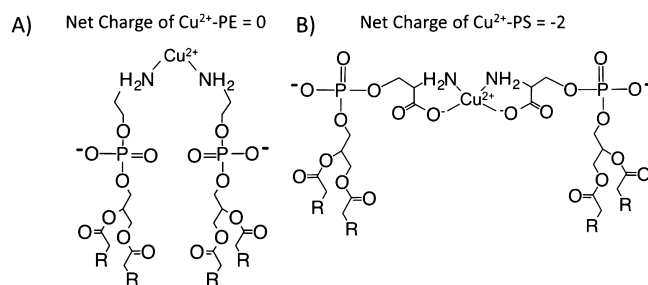


**Figure 7.** (A)  $\text{Cu}^{2+}$  binds to the amine on two PE lipids forming a bivalent complex with a net-neutral charge. (B)  $\text{Cu}^{2+}$  binds to the amine and carboxylate of two PS lipids to form a bivalent complex with a net charge of -2.

binding in these two cases is otherwise physically very different. First, the apparent affinity of  $\text{Cu}^{2+}$  for PS lipids is far tighter than that measured for PE. The  $K_{\text{DApp}}$  of  $\text{Cu}^{2+}$  for bilayers containing 10 mol % POPS is 16 pM,<sup>28</sup> which is almost 5 orders of magnitude tighter than what was found here (Table 1). This difference can be partially attributed to the negative charge on PS lipids, which does not change after metal ion binding. As shown in Figure 7, the  $\text{Cu}^{2+}$ -PE complex is neutral,

whereas the  $\text{Cu}^{2+}$ –PS complex is negatively charged. The negative surface potential of PS-containing membranes causes an increased  $\text{Cu}^{2+}$  concentration in the double layer adjacent to the membrane surface. As PE is zwitterionic at pH 7.4, the surface concentration of  $\text{Cu}^{2+}$  is identical to that of the bulk solution. After correcting for the surface potential difference in PS containing membranes, the intrinsic equilibrium dissociation constant,  $K_{\text{DInt}}$  of the  $\text{Cu}^{2+}$ –PS complex in bilayers containing 10 mol % POPS is 10 nM,<sup>28</sup> which is still 2 orders of magnitude tighter than for PE. This intrinsic difference should be the result of the fact that  $\text{Cu}^{2+}$  binds to both the carboxylate and amine on the PS headgroup as opposed to just the amine on PE. Binding to the carboxylate of the PS headgroup apparently allows  $\text{Cu}^{2+}$  to bind to the adjacent amine at pH values (pH 6.9)<sup>15</sup> far below its apparent  $\text{p}K_{\text{a}}$  (pH 11.5). In contrast, the data above show that  $\text{Cu}^{2+}$  can only bind to the amine on PE 2 pH units below its apparent  $\text{p}K_{\text{a}}$  (9.6).<sup>27</sup>

The results presented herein show that  $\text{Cu}^{2+}$  binds to the amine moiety on PE lipids and can react with  $\text{H}_2\text{O}_2$  to increase the concentration of ROS, which could, in turn, oxidize double bonds on lipid tails, adjacent to the membrane surface. The binding of other transition metal ions, including  $\text{Fe}^{2+}$ , to PE or other free amine moieties in lipid headgroups could have similar effects. Complexes between transition metal ions and lipids are reminiscent of transition metal ions bound to proteins, commonly referred to as metalloproteins. By analogy, the existence of tight binding sites with lipids suggests that metallomembranes need to be considered, which encompass the entire family of metal ion–lipid complexes and their associated chemical effects.

## ■ ASSOCIATED CONTENT

### ● Supporting Information

The Supporting Information is available free of charge on the ACS Publications website at DOI: 10.1021/jacs.5b11561.

Materials and methods section; supplementary data including quenching measurements for bilayers containing NBD-PE, DLPE lipids, and experiments in different buffers; data from DSC and FRAP experiments, binding curves at 37 °C for SLBs containing 70 mol % POPE, a Stern–Volmer plot, detailed calculations of the bilayer surface potential, and  $K_{\text{DInt}}$  values, high magnification images of PE-containing bilayers, quenching measurements as pH is cycled between high and low values, pseudo-first order reaction rates of C11-BODIPY as a function of PE content, oxidation of C11-BODIPY with lower concentrations of hydrogen peroxide, oxidation measurements of C11-BODIPY at 12 and 37 °C, and the emission spectra of C11-BODIPY in vesicles containing 40 mol % POPE and FRAP measurements of SLBs under oxidizing conditions (PDF)

## ■ AUTHOR INFORMATION

### Corresponding Author

\*pscl1@psu.edu

### Notes

The authors declare no competing financial interest.

## ■ ACKNOWLEDGMENTS

We acknowledge support from the Office of Naval Research (N00014-14-1-0792) and the National Science Foundation (CHE-1413307).

## ■ REFERENCES

- (1) Reed, T. T. *Free Radical Biol. Med.* **2011**, *51*, 1302.
- (2) Desai, V.; Kaler, S. G. *Am. J. Clin. Nutr.* **2008**, *88*, 855S.
- (3) Waggoner, D. J.; Bartnikas, T. B.; Gitlin, J. D. *Neurobiol. Dis.* **1999**, *6*, 221.
- (4) Marnett, L. J. *Toxicology* **2002**, *181*, 219.
- (5) Dix, T. A.; Aikens, J. *Chem. Res. Toxicol.* **1993**, *6*, 2.
- (6) Devos, C. H. R.; Schat, H.; Dewaal, M. A. M.; Vooijs, R.; Ernst, W. H. O. *Physiol. Plant.* **1991**, *82*, 523.
- (7) Zago, M. P.; Oteiza, P. I. *Free Radical Biol. Med.* **2001**, *31*, 266.
- (8) Chauhan, A.; Sheikh, A. M.; Chauhan, V. *Am. J. Biochem. Biotechnol.* **2008**, *4*, 95.
- (9) Girotti, A. W.; Thomas, J. P. *J. Biol. Chem.* **1984**, *259*, 1744.
- (10) Girotti, A. W.; Thomas, J. P. *Biochem. Biophys. Res. Commun.* **1984**, *118*, 474.
- (11) Hochstein, P.; Kumar, K. S.; Forman, S. J. *Ann. N. Y. Acad. Sci.* **1980**, *355*, 240.
- (12) Vance, J. E.; Tasseva, G. *Biochim. Biophys. Acta, Mol. Cell Biol. Lipids* **2013**, *1831*, 543.
- (13) Mclaughlin, A.; Lau, A.; Mclaughlin, S. *Biophys. J.* **1981**, *33*, A110.
- (14) Bergendi, L.; Benes, L.; Durackova, Z.; Ferencik, M. *Life Sci.* **1999**, *65*, 1865.
- (15) Monson, C. F.; Cong, X.; Robison, A. D.; Pace, H. P.; Liu, C. M.; Poyton, M. F.; Cremer, P. S. *J. Am. Chem. Soc.* **2012**, *134*, 7773.
- (16) Simonsson, L.; Hook, F. *Langmuir* **2012**, *28*, 10528.
- (17) Richter, R. P.; Him, J. L. K.; Tessier, B.; Tessier, C.; Brisson, A. R. *Biophys. J.* **2005**, *89*, 3372.
- (18) Wan, C.; Kiessling, V.; Cafiso, D. S.; Tamm, L. K. *Biochemistry* **2011**, *50*, 2478.
- (19) Frenkel, N.; Makky, A.; Sudji, I. R.; Wink, M.; Tanaka, M. J. *Phys. Chem. B* **2014**, *118*, 14632.
- (20) Hussain, N. F.; Siegel, A. P.; Ge, Y. F.; Jordan, R.; Naumann, C. A. *Biophys. J.* **2013**, *104*, 2212.
- (21) Pandey, A. P.; Haque, F.; Rochet, J. C.; Hovis, J. S. *Biophys. J.* **2009**, *96*, 540.
- (22) Carton, I.; Brisson, A. R.; Richter, R. P. *Anal. Chem.* **2010**, *82*, 9275.
- (23) Dietrich, C.; Bagatolli, L. A.; Volovyk, Z. N.; Thompson, N. L.; Levi, M.; Jacobson, K.; Gratton, E. *Biophys. J.* **2001**, *80*, 1417.
- (24) Axelrod, D.; Koppel, D. E.; Schlessinger, J.; Elson, E.; Webb, W. W. *Biophys. J.* **1976**, *16*, 1055.
- (25) Soumpasis, D. M. *Biophys. J.* **1983**, *41*, 95.
- (26) Cannon, B.; Hermansson, M.; Gyorke, S.; Somerharju, P.; Virtanen, J. A.; Cheng, K. H. *Biophys. J.* **2003**, *85*, 933.
- (27) Tsui, F. C.; Ojcius, D. M.; Hubbell, W. L. *Biophys. J.* **1986**, *49*, 459.
- (28) Cong, X.; Poyton, M. F.; Baxter, A. J.; Pullancherry, S.; Cremer, P. S. *J. Am. Chem. Soc.* **2015**, *137*, 7785.
- (29) Israelachvili, J. N. *Intermolecular and Surface Forces, 3rd Edition* **2011**, *1*.
- (30) Kucerka, N.; van Oosten, B.; Pan, J. J.; Heberle, F. A.; Harroun, T. A.; Katsaras, J. *J. Phys. Chem. B* **2015**, *119*, 1947.
- (31) Pham, A. N.; Xing, G. W.; Miller, C. J.; Waite, T. D. *J. Catal.* **2013**, *301*, 54.
- (32) Gutteridge, J. M. C. *FEBS Lett.* **1984**, *172*, 245.
- (33) Pap, E. H. W.; Drummen, G. P. C.; Winter, V. J.; Kooij, T. W. A.; Rijken, P.; Wirtz, K. W. A.; Op den Kamp, J. A. F.; Hage, W. J.; Post, J. A. *FEBS Lett.* **1999**, *453*, 278.
- (34) Drummen, G. P. C.; van Liebergen, L. C. M.; den Kamp, J. A. F. O.; Post, J. A. *Free Radical Biol. Med.* **2002**, *33*, S266.
- (35) Drummen, G. P. C.; Gadella, B. M.; Post, J. A.; Brouwers, J. F. *Free Radical Biol. Med.* **2004**, *36*, 1635.
- (36) Bergstrom, F.; Mikhalyov, I.; Hagglof, P.; Wortmann, R.; Ny, T.; Johansson, L. B. A. *J. Am. Chem. Soc.* **2002**, *124*, 196.
- (37) Halliwell, B.; Clement, M. V.; Long, L. H. *FEBS Lett.* **2000**, *486*, 10.
- (38) MacDonald, M. L.; Murray, I. V. J.; Axelsen, P. H. *Free Radical Biol. Med.* **2007**, *42*, 1392.

- (39) Pryor, W. A. *Annu. Rev. Physiol.* **1986**, *48*, 657.
- (40) Hicks, M.; Gebicki, J. M. *FEBS Lett.* **1986**, *199*, 92.
- (41) Sagripanti, J. L.; Kraemer, K. H. *Bull. Exp. Biol. Med.* **1989**, *264*, 1729.
- (42) Rai, P.; Cole, T. D.; Wemmer, D. E.; Linn, S. *J. Mol. Biol.* **2001**, *312*, 1089.
- (43) Rai, P.; Wemmer, D. E.; Linn, S. *Nucleic Acids Res.* **2005**, *33*, 497.
- (44) Ramirez, D. C.; Mejiba, S. E. G.; Mason, R. P. *J. Biol. Chem.* **2005**, *280*, 27402.
- (45) Hawkins, C. L.; Davies, M. J. *Biochim. Biophys. Acta, Mol. Basis Dis.* **1997**, *1360*, 84.
- (46) Dean, R. T.; Fu, S. L.; Stocker, R.; Davies, M. J. *Biochem. J.* **1997**, *324*, 1.
- (47) Stadtman, E. R.; Oliver, C. N. *J. Biol. Chem.* **1991**, *266*, 2005.
- (48) McLaughlin, S. G.; Szabo, G.; Eisenman, G. *J. Gen. Physiol.* **1971**, *58*, 667.
- (49) Schultz, Z. D.; Pazos, I. M.; McNeil-Watson, F. K.; Lewis, E. N.; Levin, I. W. *J. Phys. Chem. B* **2009**, *113*, 9932.
- (50) Boettcher, J. M.; Davis-Harrison, R. L.; Clay, M. C.; Nieuwkoop, A. J.; Ohkubo, Y. Z.; Tajkhorshid, E.; Morrissey, J. H.; Rienstra, C. M. *Biochemistry* **2011**, *50*, 2264.